

PPPL- 5069

PPPL-5069

Examination of the Entry to Burn and Burn Control for the ITER 15 MA Baseline and Other Scenarios

C.E. Kessel, S.-H. Kim, F. Koechl, V. Leonov

September 2014



Princeton Plasma Physics Laboratory

Report Disclaimers

Full Legal Disclaimer

This report was prepared as an account of work sponsored by an agency of the United States Government. Neither the United States Government nor any agency thereof, nor any of their employees, nor any of their contractors, subcontractors or their employees, makes any warranty, express or implied, or assumes any legal liability or responsibility for the accuracy, completeness, or any third party's use or the results of such use of any information, apparatus, product, or process disclosed, or represents that its use would not infringe privately owned rights. Reference herein to any specific commercial product, process, or service by trade name, trademark, manufacturer, or otherwise, does not necessarily constitute or imply its endorsement, recommendation, or favoring by the United States Government or any agency thereof or its contractors or subcontractors. The views and opinions of authors expressed herein do not necessarily state or reflect those of the United States Government or any agency thereof.

Trademark Disclaimer

Reference herein to any specific commercial product, process, or service by trade name, trademark, manufacturer, or otherwise, does not necessarily constitute or imply its endorsement, recommendation, or favoring by the United States Government or any agency thereof or its contractors or subcontractors.

PPPL Report Availability

Princeton Plasma Physics Laboratory:

<http://www.pppl.gov/techreports.cfm>

Office of Scientific and Technical Information (OSTI):

<http://www.osti.gov/scitech/>

Related Links:

[U.S. Department of Energy](#)

[Office of Scientific and Technical Information](#)

Examination of the Entry to Burn and Burn Control for the ITER 15 MA Baseline and Other Scenarios

C. E. Kessel¹, S.-H. Kim², F. Koechl³, V. Leonov⁴

¹Princeton Plasma Physics Laboratory, Princeton, New Jersey, USA

²ITER Organization, Route de Vinon-sur-Verdon, CS 90 046, 13067 St Paul Lez Durance Cedex, France

³Association EURATOM-OAW/ATI, Atominstytut, TU-Wein, Vienna, Austria

⁴NRC Kurchatov Institute, Moscow, Russia

email: ckessel@pppl.gov

Abstract. The entry to burn and flat-top burn control in ITER will be a critical need from the first DT experiments. Simulations are used to address time-dependent behavior under a range of possible conditions that include injected power level, impurity content (W, Ar, Be), density evolution, H-mode regimes, controlled parameter (W_{th} , P_{net} , P_{fusion}), and actuator (P_{aux} , fueling, f_{Ar}), with a range of transport models. A number of physics issues at the L-H transition require better understanding to project to ITER, however, simulations indicate viable control with sufficient auxiliary power (up to 73 MW), while lower powers become marginal (as low as 43 MW).

1. Introduction

ITER [1] will provide the first burning plasma with a high ratio of P_{alpha} to P_{input} of ~ 10 . The plasma will reach this regime by operating in an ELMy H-mode, which is considered a robust plasma regime based on the large database [1] of experimental tokamaks that routinely operate there. The plasma will have inductively driven current to provide high plasma current, subsequently giving high global energy confinement times, extrapolating from the present tokamak database. However, the various tokamaks around the world enter the H-mode regime with different recipes (heating power, density, in I_p ramp or flat-top), typically reach their best global energy confinement under different conditions, and may exhibit ELM-free or different ELM regimes prior to entering their steady ELMy H-mode state [2-8]. At the transition from L-mode to H-mode the temperature and density profiles form pedestals, on a fast time scale, less than or about an energy confinement time, while the characteristic rise in the central or line average density can take a few energy confinement times. In ITER, the entry to the H-mode is synonymous with the entry to the burning phase for 50/50 DT fuel mixture, since the higher energy confinement and density of H-mode significantly increases the fusion reactivity, $n_D n_T \langle \sigma v \rangle$. The power threshold for onset of the H-mode [9] is derived from a database with significant scatter among the various tokamaks, and it is clear that various features [4,7] of the plasma configuration can contribute to this scatter. In addition, the available power on ITER to robustly enter the H-mode, P_{input}/P_{thr} , is lower relative to present tokamak experiments.

The control of the flat-top burn phase is a critical demonstration for ITER, showing the simultaneous regulation of the plasma core fuel density, fusion power gain, and consistent divertor operation, under several constraints and perturbations. The impurities (Be, Ar, W), divertor detachment, multi-species core particle transport, and core energy transport will perturb the plasma burn from its reference target, making feedback control a critical feature even at the earliest DT operations. The ITPA-IOS group is doing time dependent integrated simulations (TSC [10,11], Corsica [12,13], ASTRA/ZIMPUR [14,15], and JETTO/SANCO [16,17,18]) of the burn regime in ITER to better understand the impacts of physics

uncertainties and to develop and test control strategies for the device. The baseline, hybrid and steady state scenarios are being examined.

2. Examination of Entry to Burn

The anticipated rampup phase of the baseline scenario is to remain in L-mode over all the or most of the current ramp, with a density that is feedback controlled to avoid low density issues such as tearing modes, but avoid high density that may make H-mode entry more difficult, P_{thr} (ITER, MW) [9] = $90n_L^{0.72}$. In addition, a density permissible must be met for the injection of the neutral beams (NB), of approximately $0.35 \times 10^{20} / m^3$. Some heating (5-20 MW) will be applied to reduce the volt-second consumption and control I_i , and the plasma begins sawtoothing before the end of the ramp or soon after, depending on the ramp rate and the injected power. The plasma is grown to full size and shape by half the ramp or earlier. At the end of the rampup the high power phase begins, injecting all or some combination of NB, ion cyclotron (IC), and electron cyclotron (EC) powers. The criteria to enter the H-mode is that the loss ($P_{input} - dW/dt$) or net power ($P_{input} - P_{rad} - dW/dt$) is greater than the threshold power, or some factor times the threshold power. Some experiments [4] indicate that $> 2xP_{thr}$ power is required to access the highest energy confinement, while others indicate only $\sim P_{thr}$ [5] is required. Furthermore, some experiments indicate no hysteresis [4] if the power then drops below the threshold, while others show routine hysteresis [5] without a back transition.

Simulations of the entry to burn are performed to examine the dependences on injected power, rate of rise of the density, argon or tungsten impurity timing and amount, and feedback control. The density at the end of the current rampup, can be used to reduce the power threshold, within limits to avoid resistive instabilities, however, it is found that the density rise resulting from the H-mode transition could nullify the instantaneous benefit of exceeding the threshold, by catching up with the net power, and associated dW/dt and radiation. The density rise that follows the L-H transition affects the ability to maintain the net power above the threshold with the alpha power rising as $n_D n_T$ and the threshold rising as $n^{0.72}$. The experimental database [9] indicates that the density where the minimum power is required to enter the H-mode is in the range of $n_{min}^{LH}/n_{Gr}^{flattop} \sim 0.2-0.4$, with toroidal magnetic fields over the range of 1.0-5.3 T, inferring for the ITER baseline scenario, values of $0.24-0.48 \times 10^{20} / m^3$. Since radiation is an important factor in ITER's plasma power balance it is included in the simulations, and P_{net} is used when comparing to the threshold power [2,3]. Fig. 1 shows the end of ramp (EOR) densities of $n_{20}(0) \sim 0.45$ and 0.2 for 73 MW and 43 MW of injected power, respectively, and different density rise trajectories. The 43 MW case has 0.03% Ar and 2% Be, while the 73 MW case has 0.15% Ar and 2% Be. While 73 MW was capable of entering and sustaining an H-mode regardless of the density rise trajectory, the 43 MW case was marginal unless hysteresis is present, showing the difficulty in establishing a large ratio of P_{net}/P_{thr} at the low injected power level (43 MW). These plots highlights the three phases of H-mode entry and sustainment, 1) instantaneous injection of power, 2) density rise phase, and 3) flattop relaxed phase, all of which reach some P_{net}/P_{thr} ratio. A better understanding of the density rise phase and any dependence it may have on the EOR density, and the final density in H-mode is critical to predicting the burn onset behavior. Recent experiments on JET [19] show that the temperature pedestal and density pedestal form very rapidly, while the progressive rise in the line average density is slower, on the scale of $1-3\tau_E$. It is also common on experimental tokamaks to have the H-mode begin in an ELM-free phase which transitions to an ELMy phase, however, if the ELM-free phase lasts long enough it leads to density (impurity) accumulation and a radiative collapse to L-mode. The precise

conditions leading to an ELM-free phase are not understood well enough to project to ITER, however avoiding radiative collapses in the burn phase will be necessary to avoid potential disruptions from the H-L transition at high stored energy.

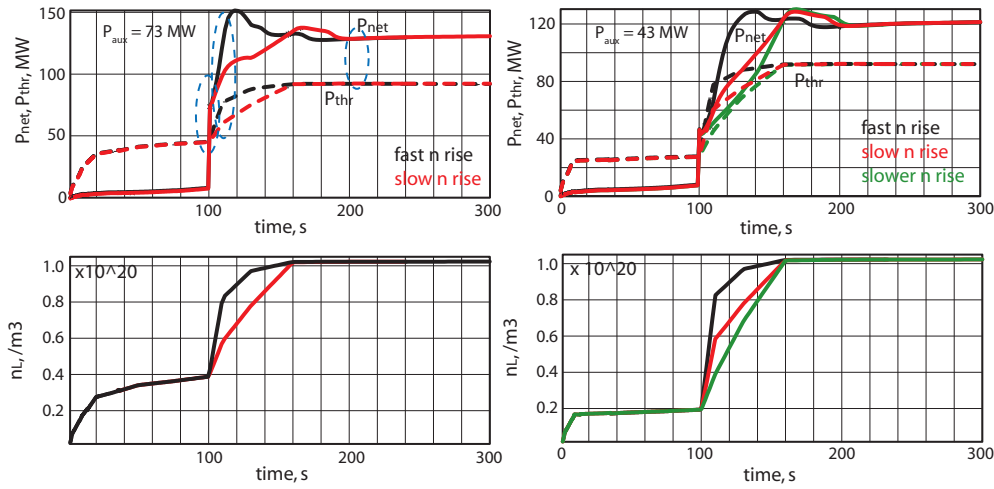


FIG 1. Net and threshold power, and electron density versus time for L-H transition assuming different end of ramp densities and density rise trajectories, with 73 and 43 MW of injected power (TSC).

In ITER, the intentional introduction of impurities will be used to radiate power from the core plasma and in the divertor, and the unintentional tungsten impurity is expected to be present from the divertor, in addition to the beryllium from the first wall. The divertor can not handle attached operation at typical plasma power exhaust levels ($P_{SOL} \sim 100$ MW) for more than a few s [20], so that the divertor must be prepared for the high power injection associated with the entry to H-mode. The divertor operating regime is targeting partial detachment which can obtain a radiated power fraction in the divertor of about 70%. Scrape-off layer plasma and neutral simulations are generally steady state solutions [21], and would provide self-consistent DT fuel, helium, and impurity densities with the power entering the divertor. There is some delay associated with the plasma stored energy rise, after high power injection to enter the H-mode, but the dynamic time-scales for divertor gasification that are consistent with the power reaching the divertor are not clear. The intentional injection of impurities (argon) and sputtered impurities (Be always present, and tungsten) from the first wall and the divertor are expected to leak into the core plasma, and this behavior is difficult to predict, although some efforts are underway to model this physics [22]. The level of the impurity, the time when it is present, and the injected power available determine the subsequent behavior at entry to burn. Simulations examining early (25s prior to EOR), medium (at EOR) and late (10 after EOR) Ar injection showed that with 73 MW of input power the earlier injection did not hinder or significantly affect the entry to H-mode, while at 43 MW of injected power the timing and amount of Ar strongly affected the access.

Shown in Fig. 2 are the line radiation profiles with electron temperature and density overlaid, and Z_{eff} and P_{net} versus time, for combinations of tungsten and argon impurities. The injected power was 73 MW, the pedestal temperature was held at 4.7 keV, and the impurity profiles are the same as the electron profile. The argon dominantly radiates near the plasma separatrix and somewhat deeper into the plasma core, while tungsten radiates strongly throughout the outer 1/3 of the plasma, and strongly in the pedestal region. The tungsten radiation can collapse the pedestal region and create a cold front that penetrates deeper into

the plasma core. The three cases shown have similar P_{net} values, while their Z_{eff} 's are very different.

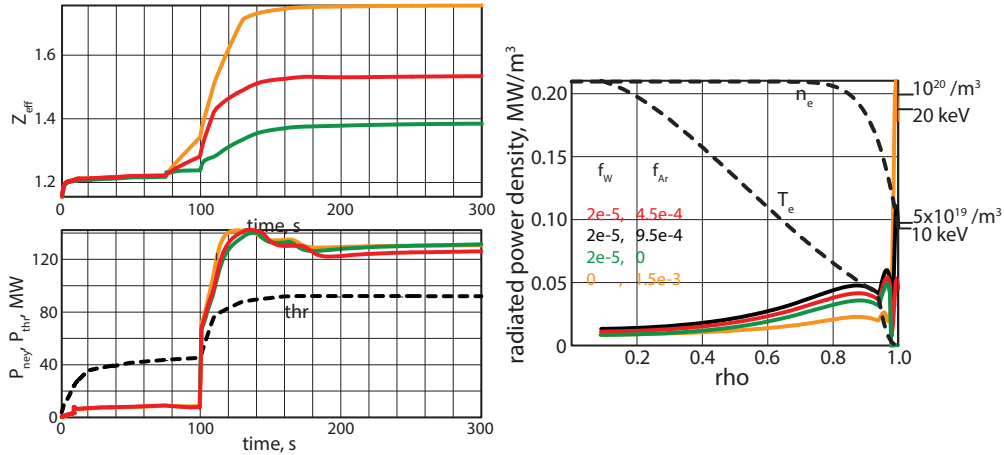


FIG 2. Simulations of 73 MW of injected power at the LH transition, with varying Ar and W impurity concentrations, with 2% Be, showing the line radiated power and corresponding Z_{eff} , all reaching about the same level of net (SOL) power (TSC).

For the baseline scenario at 15 MA, assuming the W is distributed like the electron profile, multiple codes found tungsten concentrations relative to electrons of $\sim 2\text{--}4 \times 10^{-5}$ resulted in radiative collapses in most cases depending on the amounts of Be and Ar included. Fig. 3 shows the L-H transition and relaxed flattop phases for a case with $n_{\text{Be}}/n_e = 5.5\%$ and $n_{\text{W}}/n_e = 5.5 \times 10^{-7}$, and 3.8% and 3.8×10^{-5} , respectively. The higher tungsten case collapses when the total radiation reaches 57 MW bringing the net power below the threshold power. Also shown is a successful rampdown with Be and Ar impurities, maintaining the net power above the threshold for 85 s until the power is dropped to back transition to L-mode. The rampdown is a critical discharge phase to avoid impurity accumulation and a back transition too early. Experiments on C-Mod [23] showed that maintaining sufficient auxiliary power can avoid accumulation of Mo, and the radiated power dropped with the plasma current and density in both H-mode and L-mode.

3. Simulation of Flattop Burn Control

Although the entry to burn may be a combination of pre-programming and feedback control, the flattop burn phase will largely be regulation of a burning set point. Various quantities of interest can be feedback controlled, such as the plasma stored energy, the power entering the scrape-off layer, the ratio of $P_{\text{net}}/P_{\text{thr}}$, or the fusion gain, for example. The primary actuators are the auxiliary heating power and the plasma density [24] (including impurities), however, power is symmetric on and off with fast time scales, while particles can be introduced quickly but removed only slowly. More sophisticated tools manipulating energy confinement can also be envisioned, however, they are not as direct as heating and may have complex interactions. The feedback control system requires measurements (and/or interpretive signals), controlled parameters, actuators to facilitate that control, and an understanding of limits to control, anticipated disturbances, and various physical time-scales [25].

The plasma stored energy was feedback controlled with auxiliary power, prescribing the density evolution, and using Coppi-Tang (CT) semi-empirical and GLF23 energy transport for comparison. Both cases obtain ~ 100 MW of alpha power with 68 MW of auxiliary power,

about 29 MW of line, 20 MW of bremsstrahlung, and 4 MW of cyclotron radiation losses. The pedestal temperatures are both at 4.8 keV as predicted by EPED1, while the CT model has a broader temperature profile than the GLF. The $f_w = 0.002\%$, $f_{Ar} = 0.05\%$, and $f_{Be} = 2\%$.

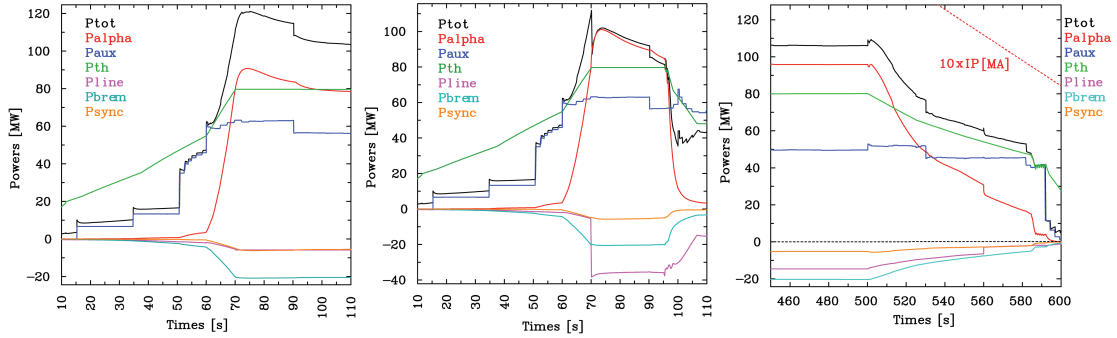


FIG. 3. The powers into and radiated from the plasma for a case with high Be and low W, and a case with high Be and high W, the latter collapses due to strong line radiation from the W. The rampdown phase is also shown for an Ar and Be impurity mix, maintaining H-mode for 85s (Corsica).

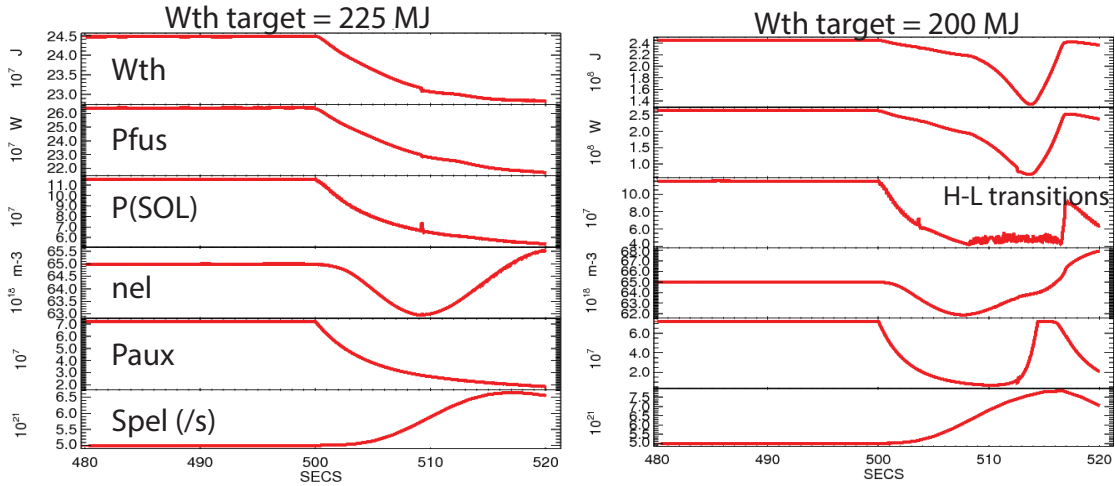


FIG. 4. Stored energy feedback simulations for a hybrid scenario at 12.5 MA, with density control on the line average density, with Be and W impurities. The lower stored energy case resulted in too little auxiliary power to compensate the radiation losses, and the target could not be reached (JETTO/SANCO).

The actual ELMy H-mode regime accessed may be partially understood in terms of peeling-ballooning theory [26], however, this does not directly predict the regime. JET [4] has specific requirements to reach Type I ELMy H-mode with $H_{98} \sim 1.0$, with $P_{\text{loss}}/P_{\text{thr}} > 2.2$, while lower values access lower confinement, have ELM-free phases, or lower confinement type III ELMy regimes. No hysteresis is observed either. Meanwhile, AUG [5] can access the $H_{98} \sim 1$ type I ELMy regime with $P_{\text{loss}} \geq P_{\text{thr}}$, and hysteresis is observed. Simulations were done to examine the impact of a multi-regime H-mode for ITER by considering type I ELMy H-mode for $P_{\text{net}}/P_{\text{thr}} \geq 1.3$ with $H_{98} = 1$, type III ELMy H-mode with $H_{98} = 0.8$ for $0.5 < P_{\text{net}}/P_{\text{thr}} < 1.3$, and hysteresis that maintains $H_{98} = 0.8$ until $P_{\text{net}}/P_{\text{thr}} < 0.5$ where H_{98} drops to 0.5 (L-mode). This showed that with a maximum of 73 MW of input power and 0.15% argon fraction, the plasma could enter type I ELMy H-mode and remain there, while 63 MW or less would drop back to type III H-mode, and 53 MW would drop back to L-mode. Reducing the argon fraction to 0.1% allowed the 53 MW cases to remain in type III H-mode. Assuming 0.0015% tungsten and 0.05% argon, resulted in a type I ELMy H-mode with 73 MW of injected power, while if the tungsten reached 0.00176%, the plasma entered the type I regime and later

dropped all the way to L-mode with a radiative collapse of the plasma. The tungsten leads to significantly greater sensitivity than argon, where radiative collapses end in L-mode rather than a transition just to type III ELM regime. This raises questions about how to diagnose an excessive level of impurity in ITER, either unintentional such as tungsten, or intentional such as argon, via radiation level or rate of change of radiation level. Using auxiliary power to compensate higher radiation around the L-H transition time will be hindered due to the need for all or a large fraction of the power just to enter the higher confinement H-mode regime. Some power may need to be diverted for neo-classical tearing mode or sawtooth control, reducing the available power for bulk heating. Examining the available diagnostics [26] in the machine protection and basic control groups, the real-time capability of these systems will need to be determined. The long time scale of particle residence in the plasma chamber makes rapid response difficult, so that some forward projections are needed to anticipate the impact of impurities on the given plasma state. It is not known if ITER will have similar H-mode regimes and requirements to reach the highest confinement as seen in JET. Better understanding of why these regimes exist and what conditions produce them is needed in order to guarantee ITER's entry and sustainment of high confinement H-mode.

Simulations were also done introducing slow changes in the requested stored energy, argon concentration, and energy confinement, showing good tracking behavior. Here GLF23 was used for the energy transport in the H-mode phase. A set-point of $W_{th} = 390$ MJ dropping to 310 MJ, and then rising back again to 390. The argon fraction starts at 0.05%, rises to 0.2% and drops to 0.15%. The use of the scrape-off layer power as the controlled variable was also demonstrated, with the actuator still the auxiliary power, at different argon fractions. Additional simulations demonstrated the use of the pellet fueling rate to alter the flattop plasma density, simultaneously with stored energy feedback at 370 MJ.

The hybrid scenario at 12.5 MA and $n/n_{Gr} = 0.65$, is also examined for feedback control of the plasma stored energy, fusion power and scrape-off layer (or net) power through the variation of auxiliary power. Pellet injection is used to maintain a plasma density level. Bohm-gyroBohm and GLF23 are used for energy transport, with impurity transport included. Fig. 4 shows simulations of feedback control of the stored energy to two different target values. While the larger value is controlled well, the lower value is difficult to reach since the net power drops to the threshold power causing H-L transitions. Scrape-off layer power feedback control, with P_{aux} , was examined with long time drift in tungsten concentration, showing good control for $P_{SOL} = 90$ MW. Simulations of the hybrid entry to burn showed the impact of s/q on the fusion gain accessible, length of flattop time with $q > 1$, and effects of toroidal rotation on improving performance, and the density rise time.

Simulations of a steady state scenario in flattop were carried out with simultaneous multi-variable feedback control of the main parameters to demonstrate the possibility of simplified and robust control of these parameters using only integral characteristics of plasma without detail control of radial profiles. As a test perturbation a sudden doubling of the beryllium impurity flux from the wall was introduced. Fig. 5 shows transient responses of parameters in time dependent fix boundary simulations using transport code ASTRA [16] with scaling-based plasma transport model and impurity code ZIMPUR [17]. This modelling confirms that in spite of occasional conflicting conditions for different control channels, the diagonal version of the controller using a simple astatic control law could be effective (control the plasma density by fueling, the fusion power by NB injection, the loop voltage with lower

hybrid current drive power (P_{LH}), and power flux into the SOL and divertor (P_{loss}) by argon seeding). The left column of fig. 5 corresponds to the case when the system has closed loop feedback. The open-loop scheme case is depicted in the right column. This demonstrates that stabilization of plasma parameters relative to their references after strong enough perturbation (which results in plasma full cooling at open feedback loops) can be realized. Simulations of similar perturbations were examined also at high Q, all showing good plasma controllability.

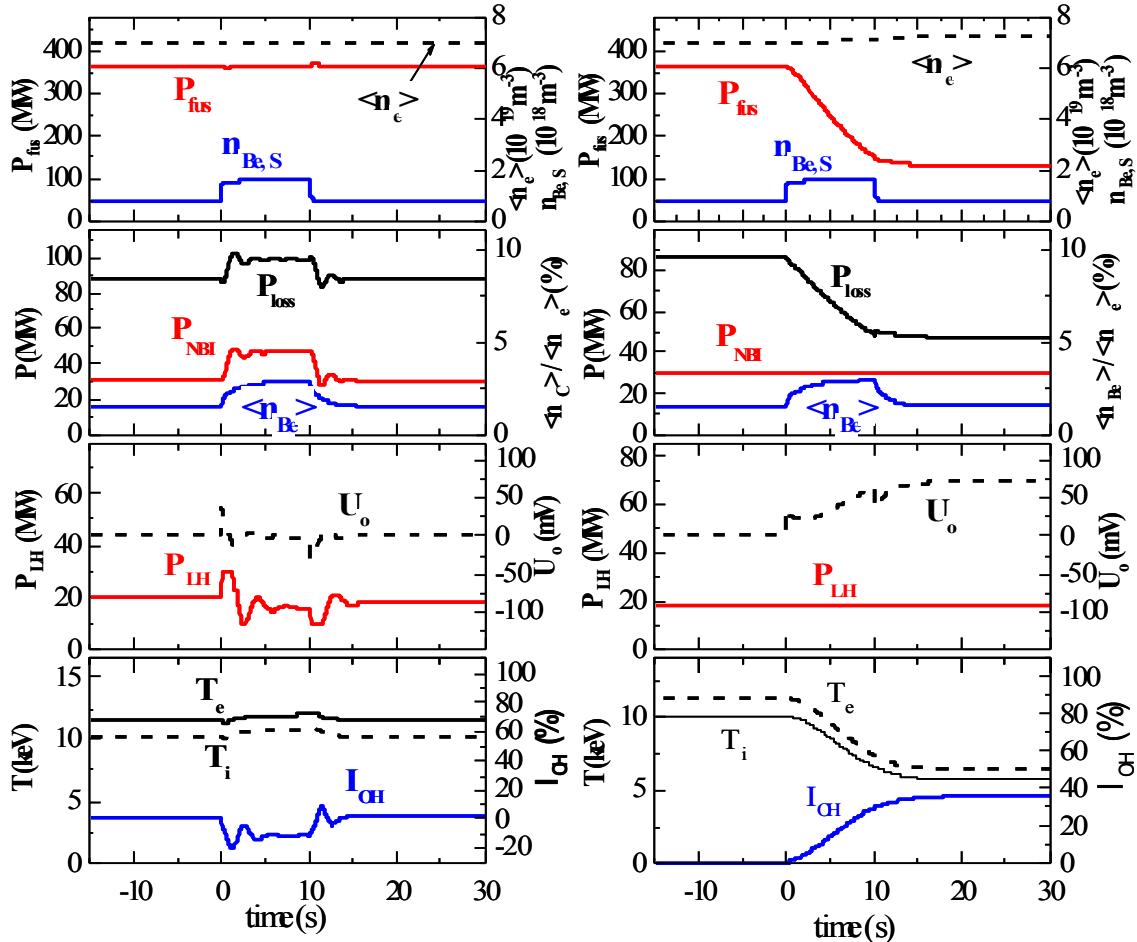


FIG. 5 Plasma parameters response at doubling of Be impurity flux to the plasma boundary, with feedback control on left, and open loop on the right (ASTRA/ZIMPUR).

4. Observations and Future Work

The ITPA-IOS group is examining the entry to burn and burn control for ITER scenarios presently focusing on global parameter feedback. A entry to burn is complicated by physics behavior that is not well understood, including the L to H threshold energy, the H-mode regimes (e.g. ELM-free, Type I, Type III) and corresponding energy confinement, the density rise phase, particle screening, hysteresis in H-mode, and behavior of impurities (particularly tungsten and argon) and their impacts. Dedicated experiments to address these aspects should improve projections for ITER. Access to 73 MW of injected power at the L-H transition provides a robust entry and relaxation under a wide range of conditions, while powers as low as 43 MW are marginalized by impurity radiation, the need for low density at end of ramp, and the trajectory of the density rise in H-mode. The rampdown has also been examined and simulations show reasonable behavior in maintaining H-mode over part of this phase and transitioning to L-mode for the remainder. Feedback control on the plasma density,

stored energy, scrape-off layer (or net) power, fusion power, as well as simultaneous multiple parameter control has been shown to be viable with a range of simulations tools and their associated models. These simulations have examined the impacts of differing impurity levels, H-mode regimes, slow and fast setpoint requests, and impurity disturbances. Details of the feedback such as measurement time delay and actuator response have not yet been included. Simulations show that there is a need to assess the state of the burn, such as radiated power and its gradient, impurity content and its gradients, relative terms like alpha power, auxiliary power and radiated power, and the viability of control actions (can they reach their target). Future work will expand the modeling treatments, include more feedback control constraints, and incorporate experimental observations for complex physics behavior.

This work is partially supported by the US Department of Energy under DE-AC02-CH0911466. The views and opinions expressed herein do not necessarily reflect those of the ITER Organization.

References

- [1] ITER Physics Basis Nucl Fusion **39** (1999); K. Ikeda et al Progress in the ITER Physics Basis **47** (2007).
- [2] J. W. HUGHES et al Nucl. Fusion **51** (2011) 083007.
- [3] C. F. MAGGI et al Nucl. Fusion **54** (2014) 023007.
- [4] Y. ANDREWS et al Phys Plas Control Fusion **50** (2008) 124053.
- [5] F. RYTER et al J Phys Conf Series **123** (2008) 012035.
- [6] A. E. HUBBARD et al Plas Phys Control Fusion **40** (1998) 689.
- [7] Y. MA et al Nucl Fusion **52** (2012) 23010.
- [8] T. N. CARLSTROM and R. J. GROEBNER Plasma Phys **3** (1996) 1867.
- [9] Y. R. MARTIN et al J. Phys Conf Series **123** (2008) 012033.
- [10] S. C. JARDIN et al J. Comput Phys **66** (1986) 481.
- [11] C. E. KESSEL et al Nucl Fusion **47** (2007) 1274.
- [12] T. CASPER et al, Nucl Fusion **54**, (2014) 013005.
- [13] S.H. KIM et al, CORSICA Modelling of ITER Hybrid Mode Operation Scenarios, 24th Int. Conf. on Fusion Energy (San Diego, USA) ITR/P1-13 (2012).
- [14] PEREVERZEV, G.V., YUSHMANOV, P.N., Preprint IPP 5/98 2002, Garching. Germany.
- [15] LEONOV, V.M., ZHOGOLEV, V.E., Plasma Phys. Control. Fusion, **47** (2005) 903.
- [16] M. ROMANELLI et al Plasma and Fus Res **9** (2014) 3403023.
- [17] V. PARAIL et al Nucl Fusion **53** (2013) 113002.
- [18] F. KOEHL et al, IAEA FEC2014, this conference.
- [19] A. LOARTE et al Nucl Fusion **53** (2013) 083031.
- [20] R. A. PITTS et al J. Nucl. Mater. **415** (2011) S957.
- [21] A. S. KUKUSHKIN et al Nucl Fusion **43** (2003) 716.
- [22] V. PARAIL et al, "Coupled core-SOL modeling of W contamination in H-mode JET plasmas with ITER-like wall", accepted for publication in J Nucl Mater. 2014.
- [23] C. E. KESSEL et al Nucl Fusion **53** (2013) 093021.
- [24] E. SCHUSTER et al Fus Sci Technol. **43** (2002) 18.
- [25] J. A. SNIPES et al Fusion Eng. Des. **87** (2012) 1900.
- [26] P. SNYDER et al Plas Phys Control Fusion **46** (2004) A131.

Princeton Plasma Physics Laboratory Office of Reports and Publications

Managed by
Princeton University

under contract with the
U.S. Department of Energy
(DE-AC02-09CH11466)

P.O. Box 451, Princeton, NJ 08543
Phone: 609-243-2245
Fax: 609-243-2751

E-mail: publications@pppl.gov

Website: <http://www.pppl.gov>